Study of Adsorption of Methylene Blue onto Activated Carbon from Lignite

K. Mahmoudi*, N. Hamdi, E. Srasra

Physical Chemistry Laboratory for Mineral Materials and Their Applications,
National Center for Research in Materials Sciences (CNRSM), B.P.73 – 8020, Soliman-Tunisia
** e-mail: mahmoudikhaled1984@gmail.com*

An adsorbent has been prepared from lignite by chemical activation using $ZnCl_2$. Pore properties of the activated carbon such as the surface area determined by the Brunauer-Emmett-Teller (BET) method, pore volume, pore size distribution, and pore diameter were characterized by *t*-plot based on N_2 adsorption isotherm. The determined surface area of the adsorbent which was primarily contributed by micropores was 600 m^2/g. Activated carbon from lignite was used to adsorb methylene blue (MB) from an aqueous solution. The effects of the initial dye concentration, agitation time and initial pH have been studied. It was found that the adsorption isotherms followed both Langmuir and Freundlich models. However, the Langmuir model gave a better fit to all adsorption isotherms than the Freundlich one. The kinetics of adsorption of MB has been tested using pseudo-first-order, pseudo-second-order models, as well as the intra-particle diffusion equation. The results obtained show that the adsorption of MB from an aqueous solution onto microporous activated carbon takes place according to the pseudo-second-order model.

Keywords: activated carbon, lignite, adsorption, methylene blue.

УДК 676.164

INTRODUCTION

As the demand for environmental protection increases every year, activated carbons are extensively widely used in industry for purification, separation, and recovery processes. Activated carbon is one of the most widely used materials in water purification because of its tremendous adsorptive capacity due to a large surface area, microporosity, and good corrosion resistance. In general, preparation of activated carbon is commonly realized by chemical or physical activation. Chemical activation can be accomplished in a single step by carrying out thermal decomposition of a raw material with chemical reagents. Chemical activation processes have been carried out with acidic reagents: $ZnCl_2$ [1], H_2SO_4 [2], and H_3PO_4 [3], or with basic reagents: K_2CO_3 [4], KOH [5], NaOH [6], and Na_2CO_3 [7]. It involves pyrolyzing the feedstock in the presence of a chemical activating agent such as H_3PO_4, $ZnCl_2$, KOH, etc.

Regarding the environmental effect and chemical recovery of those agents, $ZnCl_2$ is the most preferred one. Several researchers have reported the preparation of chemically activated carbons from various raw materials, such as lignine [1], rice [8], olive stones [9], date pits [10], etc. Those materials were particularly chosen to prepare activated carbon due to the presence of high wood fiber content in them. A surface activation technique helps to develop a large superficial area, several surface functions, and the affinity for several adsorbates, but it is expensive. Lignite, used in the present investigation, is an inexpensive, low-rank carbonaceous material with a low heating value.

In the present study, activated carbon from lignite was produced using chemical activation processes. The aim was to investigate the optimum conditions for removing methylene blue (MB) and to calculate the adsorption capacity. In addition, the adsorption mechanism was investigated through two adsorption kinetic models such as the pseudo-first-order model and the pseudo-second-order model.

EXPERIMENTAL

Adsorbate

As the model adsorbate, a cationic dye which is difficult to be degraded in natural environments was selected. A standard stock solution was prepared by dissolving the dye in double distilled water to the concentration of 1000 mg/L.

Working solutions of the desired concentrations were obtained by successive dilutions.

Preparation of activated carbon

The starting lignite was washed with water several times and then dried at 423K. The dried lignite was crushed and sieved, the fractions of the particle size between 0.5 and 1.0 mm being used for the preparation of activated carbon.

The activated carbon sample was produced by chemical activation with zinc chloride (99%) and lignite, from Tunisia (from Tabarka – a coastal town located in north-western Tunisia). Lignite was added to $ZnCl_2$ grains with an impregnant/precursor mass ratio of 2 (20 g/10 g) and was mixed until the total homogeneity. The mixture of natural lignite and the activated reagent ($ZnCl_2$) was heated up to different

© Mahmoudi K., Hamdi N., Srasra E., Электронная обработка материалов, 2015, **51**(5), 16–22.

final carbonization temperatures in the same furnace at the rate of 10°/min (the activation temperature varied over the range of 300–500°C). A low temperature ramp rate was used to minimize the temperature difference between the mixture and the furnace, to provide sufficient activation time and to avoid a rapid decomposition of the sample. The sample was cooled below 323K before being removed from the furnace. After cooling to room temperature, the activation mixture was washed with hot distilled water several times so as to remove the residual chemical activating agent.

After washing, the sample was dried at 80°C in a vacuum oven for least 2 h in order to obtain activated carbon.

Instrumentation

The spectrophotometric determination of dye was done on a Shimadzu UV–vis spectrophotometer (Model UV-2100S). The pH of the solutions was measured by a microprocessor-based pH meter pH 211. The Brunauer-Emmett-Teller (BET) method was used to determine the surface area and porosity of the adsorbents. The pore size distribution, surface area (S_{BET}), micro pore volume (V_{micro}) and the total pore volume (V_{TOT}) of the produced carbon were determined from the nitrogen adsorption-desorption isotherm at 77K using a Quantachrome Autosorb 1-MP. S_{BET} was determined by the BET method as in [11] and the *t*-plot method was used to estimate the volumes of micropores and the micropore surface area. The total pore volume (V_p) was estimated from the amount of nitrogen adsorbed at a relative pressure of P/P_0 = 0.97 and the average pore diameter was calculated from $D_p = 4V_p/S_{BET}$ [12].

The Dubinin-Radushkevich equation

The Dubinin-Radushkevich (DR) equation is usually used to describe adsorption in microporous materials, especially those of a carbonaceous origin, which are the objects of the present paper. In its basic form, the DR equation can be written as:

$$W/W_0 = \exp[-(A/E)^2] = \exp[-(RT \ln (x)/E)^2],$$

where $x = p/p_0$. The characteristic energy E for a given fluid–solid system can be further expressed using a scaling factor J as:

$$E = \beta E_{0,}$$

where E_0 is the characteristic energy of a "standard" adsorbate with respect to the given solid. The characteristic curve of a system is established by plotting the logarithm of the amount adsorbed W vs $\log^2(1/x)$. This is to test the suitability of the equation and/or to determine its range of applicability. If the equation is applicable, the plot would be a straight line with a slope $(RT/E)^2$ and an intercept $\log(W_0)$, depicting the characteristic energy and the micropore volume that can be obtained.

The point of zero charge is pH at which the surface has a zero net charge, known as pH_{pzc}. It is characteristic of amphoteric surfaces and is determined by the type of surface sites on solids and their structures. The samples of powders (0.15 g) with 50 mL of 0.01M NaCl solution were shaken in the bottle for 48 h. The initial pH values were adjusted (in the pH range from 3.5 to 10) by adding a small amount of HCl or NaOH solution keeping the ionic strength constant. The final pH was measured after 48 h under agitation at room temperature. The pH_{pzc} of the adsorbent is the point where the curve pH_{final} vs $pH_{initial}$ crosses the line $pH_{initial} = pH_{final}$ [13, 14].

The amounts of acidic functional groups were determined by Boehm's method of titration with basic solutions of different base strengths: $NaHCO_3$, Na_2CO_3, NaOH, C_2H_5ONa [15, 16]. This was achieved by accurately weighing 1.00 g of the sample into four conical flasks with a stopper.

For this purpose the samples were agitated for at least 16 h with 0.05 N solutions of four bases. The amount of Na+ ions remaining in the solution iwa determined by adding an excess of the standard HCl and back-titration. The basic group contents of the oxidized samples were determined with 0.05 N HCl [16, 17].

Adsorption experiments

Adsorption studies were conducted in order to investigate the effect of pH, the effect of the contact time, and of the initial dye concentration on carbon samples.

The batch sorption studies were conducted in a set of 250 ml Erlenmeyer flasks containing 0.10 g adsorbent and 200 mL of the dye solutions with various initial concentrations: 50, 250, 500, 750, 850, and 1000 mg/L. The flasks were agitated in an isothermal shaker at 200 rpm and 30°C until the equilibrium was reached. Dye concentrations in the supernatant solutions were measured by the Lambda Bio 20 UV/Visible spectrophotometer at 664 nm for the MB uptake at equilibrium; q_e (mg/g), was determined by:

$$q_e = \frac{(C_0 - C_e) \cdot V}{W},$$

where C_0 and C_e (mg/L) are the liquid-phase concentrations of MB at initial and equilibrium, respectively, V (L) is the volume of the solution, and W (g) is the mass of adsorbent used. The effect of pH on dye removal was examined by varying the pH of the solution from 2 to 12, with the initial dye concentration of 1000 mg/L, the activated carbon from lignite dosage of 0.10 g/500 mL, and the adsorption temperature of 30°C. The initial pH of the dye solution

was adjusted by adding 0.10M of HCl or NaOH solution.

The equilibrium data were fitted using the Langmuir and Freundlich isotherm models.

The Langmuir isotherm assumes monolayer adsorption onto a surface containing a finite number of adsorption sites. The linear form of the Langmuir isotherm equation is derived in [20]:

$$\frac{C_e}{q_e} = \frac{1}{Q_0 K_L} + \frac{1}{Q_0} C_e,$$

where Q_0 (mg/g) and K_L (dm^3/g) are Langmuir constants related to the adsorption capacity and the rate of adsorption.

The Freundlich isotherm assumes heterogeneous surface energies, in which the energy term in the Langmuir equation varies as a function of the surface coverage. The well-known logarithmic form of the Freundlich isotherm is given in [21]:

$$\ln q_e = \ln K_F + \frac{1}{n} \ln C_e,$$

where K_F (mg/g) (L/mg) and 1/n are the Freundlich adsorption constant and a measure of adsorption intensity, respectively.

The procedure of adsorption kinetic was identical to the adsorption equilibrium where the aqueous samples were withdrawn at different time intervals and the concentrations of dyes were similarly measured. The amount of adsorption at time t, q_t (mg/g), was calculated by:

$$q_t = \frac{(C_0 - C_t)V}{w},$$

where C_t (mg/l) is the liquid-phase concentration of a dye at time t. When adsorption is preceded by diffusion through a boundary, the kinetics in most systems follows the pseudo-first-order equation. The first-order expression based on the solid capacity is defined in [22] as:

$$\ln\left(\frac{q_e}{q_e - q_t}\right) = \frac{k_1}{2{,}303} t,$$

where k_1(1/h) is the adsorption rate constant. Unlike the pseudo first-order equation, the pseudo second-order equation, as in [23], predicts the behavior over a whole range of adsorption and is represented as:

$$\frac{1}{(q_e - q_t)} = \frac{1}{q_e} + k_2 t,$$

where k_2 (g/mg·h) is the adsorption rate constant of the pseudo second-order equation.

RESULTS AND DISCUSSION

Characterization of the prepared adsorbent

Figure 1 shows the N_2 adsorption isotherm of activated carbon produced at the carbonization at 300, 400, 450, and 500°C using $ZnCl_2$ as reagent. It is evident from the nature of plots that N_2 adsorption follows isotherm of the type I pattern, characteristics of microporous solids according to the IUPAC classification [24]. Table 1 contains the BET surface area (S_{BET}), the external surface area (including mesopores and macropores area S_{ext}), the micropores surface area (S_{mic}), the total pore volume (V_t), and the average pore diameter (D_p), which are the results obtained by applying the BET equation to the N_2 adsorption at 77K and the DR equation to the N_2 adsorption at 77K.

It was found that the activated carbon at 450°C had a remarkable BET surface area, which was primarily contributed by micropores.

The average pore diameter was 2.6 nm, indicative of its micropores character.

It appears that activated carbon was dominantly micropores. Percentage of micropores area is 82%.

The characteristic energy (E), the micropore surface (Sμ), and the micropore volume (Vμ) of the samples studied are presented in Table 1. These values are obtained by the DR equation.

The surface micropore volume values are in the range 0–492 m^2/g. The dimensionless energy of adsorption E ranges from 5 to 6.1 kJ/mol for different samples.

As the surface acidity of carbon increased by chloride zinc activation, its pH_{pzc} was lowered, whereas heat activation at 450°C had a higher value (Table 2). The pH_{pzc} is closely related to the change of acidic or basic properties of carbon (Table 2).

The FTIR spectra of the natural lignite and lignite at 300°C, 400°C, 450°C, and 500°C (all samples were analyzed before adsorption) are given in Figure 2. The spectra present most intense peaks, indicating a relatively high concentration of the relevant functional groups. The broad band between 3200 and 3500 cm^{-1} can be attributed to -OH stretching vibration of the hydroxyl group. Low absorbance at 2923 and 2855 cm^{-1} corresponds to the C-H stretching of methylene group. The band at 1625 cm^{-1} is assigned to the C=O stretching vibrations of quinoid structure [18]. The absorbance at 1400 and 1033 cm^{-1} arises from the C-O stretching and O-H bending [19]. The presence of peaks at 526 and 473 cm^{-1} is C-C out of plane bending of aliphatic groups.

Effect of initial pH on adsorption

The magnitude of electrostatic charges imparted by the ionized dye molecules is primarily controlled by the pH of the medium. The amount of the dye adsorbed or the rate of adsorption tends to vary with pH of the aqueous medium.

The experimental results of the adsorption of MB on the natural lignite and corresponding activated carbon as a function of pH at an initial dye concentration of 1000 mg/L and 0.1 g adsorbent dosage is shown in Figure 3.

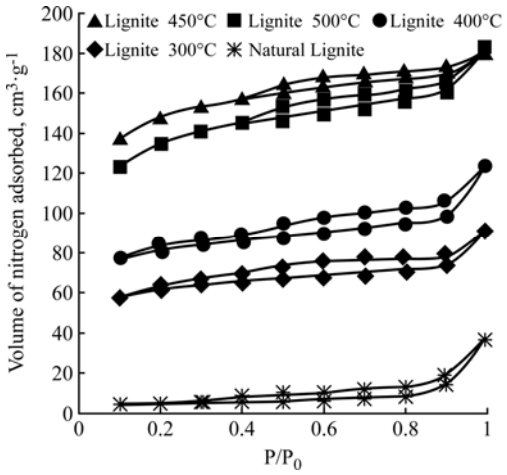

Fig. 1. Nitrogen adsorption isotherms for various activated lignite carbon samples against that of untreated lignite sample.

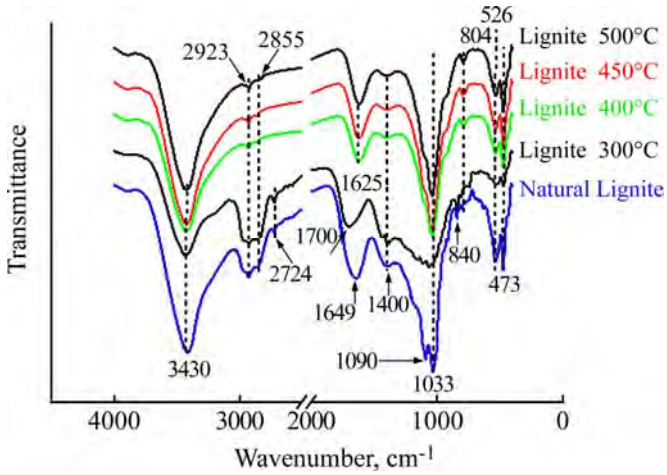

Fig. 2. FTIR spectra of raw lignite and adsorbents prepared by chemical and thermal activation.

Table 1. Physical properties of natural lignite and theirs corresponding activated carbons

	S_{BET} (m^2/g)	V_t (cm^3/g)	D_p (nm)	D-R Values		
				$S\mu$(m^2/g)	$V\mu$(cm^3g^{-1})	E(kJ/mol)
Natural lignite	12	0.11	36	0	0	1.1
Lignite 300°C	120	0.16	5.3	98	0.1	5.6
Lignite 400°C	400	0.32	3.2	328	0.19	5.8
Lignite 450°C	600	0.39	2.6	492	0.26	6.1
Lignite 500°C	495	0.34	2.7	406	0.21	6

Table 2. Chemical properties of natural lignite and their corresponding activated carbon

	pH_{pzc}	Total acid (mmol/g)	Total basic (mmol/g)
Natural lignite	4	5.17	0.8
Lignite 300°C	5.3	5.3	0.75
Lignite 400°C	5.5	5.6	0.73
Lignite 450°C	5.9	6	0.70
Lignite 500°C	5.7	5.9	0.71

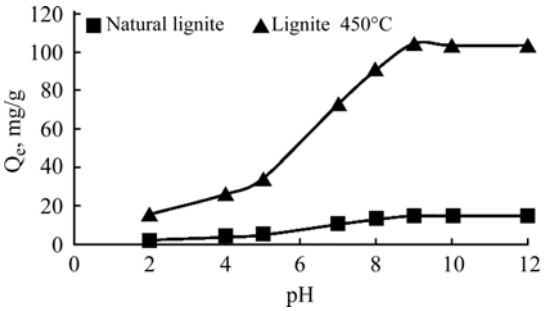

Fig. 3. Effects of solution pH on the adsorptive uptake of MB at 30°C.

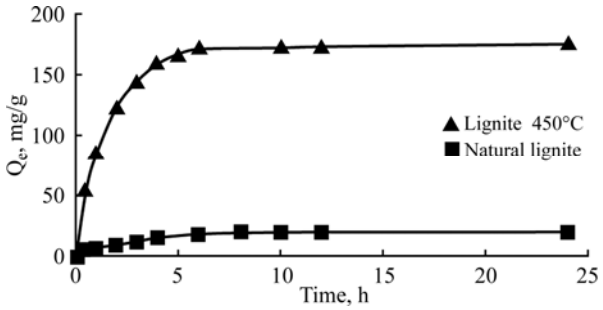

Fig. 4. Adsorption of MB on natural lignite and activated carbon as a function of contact time.

The adsorption behavior of dyes was strongly pH dependent. The highest MB adsorption capacity was experimentally observed at pH 9, this capacity drastically decreased at lower pH values. The reduction of MB removal at pH values about 9 may be ascribed to the increasing repulsive forces between the surface functional groups of AC and MB, which mainly exist as cations. These results are consistent with the data in literature [25].

Effect of contact time on adsorption

Adsorption experiments were carried out for different contact times and with a fixed adsorbent dosage of 0.1 g at pH = 9. The results in Fig. 4 rep-

Table 3. Isotherms parameters obtained by Langmuir and Freundlich models for removal of MB by activated carbon and natural lignite

Adsorbent	Langmuir Constant			Freundlich Constant		
	K_L (L/mg)	Q_e(mg/g)	R^2	1/n	K_F (mg/g)	R^2
Natural lignite	0.487	43.2	0.997	0.323	13.5	0.92
Lignite 450°C	0.106	370.37	0.994	0.39	49.8	0.858

Table 4. Kinetic parameters for the adsorption of MB onto natural lignite before and after activation at 25°C

Adsorbent	$Q_{e.exp}$ (mg/g)	First-order kinetic model			Second-order kinetic model		
		k_1 ($l \cdot g^{-1} \cdot h^{-1}$)	$Q_{e,calc}$ (mg/g)	R^2	k_2 ($g \cdot mg^{-1} \cdot h^{-1}$)	$Q_{e,calc}$ (mg/g)	R^2
Natural lignite	25	0.482	2.72	0.509	0.117	25.57	0.999
Lignite 450°C	175	0.759	22.5	0.664	0.18	178.57	0.999

resent the adsorption capacity of MB on activated carbon at different contact times as compared to natural lignite that was not carbonized.

For activated carbon from lignite at 450°C, an adsorption capacity of 178 mg/g is obtained at the 6 h contact time, 0.5 g/L adsorbent dose, and pH = 9 for MB. But the maximum adsorption capacity of natural lignite was observed at 25 mg/g for MB at 4 h. Figure 4 also shows that a rapid increase of the MB capacity is achieved during the first hour.

Adsorption isotherms

The adsorption equilibrium data were fitted for the Langmuir and Freundlich isotherms.

The isotherm results indicate that the adsorption of MB onto natural lignite and corresponding activated carbon is consistent with the Langmuir and Freundlich isotherms.

The characteristic parameters of different models as well as the correlation coefficients R^2 are listed in Table 3.

The correlation coefficients calculated for the Langmuir equation fitting are slightly_lower than those obtained in the case of the Freundlich equation. However, we think that the Langmuir model is a better description of the experimental system for the present research because the experimental data reaches a saturation plateau at high C_e. This saturation tendency is not included in the Freundlich model.

Adsorption kinetics

Kinetic parameters for the two kinetic models and correlation coefficient are summarized in Table 4.

Table 4 shows that the correlation coefficients of the second-order kinetic model are higher than others. Also, the calculated q_e values very well agree with the experimental data ($q_{e\ exp}$). These indicate that the adsorption perfectly complies with the pseudo-second-order reaction as in [26]. Similar kinetic results have been also reported in literature [27–29].

Adsorption mechanism

The adsorption mechanism for the dyes adsorption is electrostatic interaction; the removal capacity of MB is at a maximum within the range of pH 8–9. In this pH range, the surface of activated carbon is negatively charged and MB is positively charged ($-S^+$). The deprotonated groups of activated carbon are mainly carboxylic ($-CO-O^-$) and phenolic ($-O^-$) groups. At the solution pH ≥ 4, the removal capacity of MB was expected to increase, as the adsorbent was negatively charged and dye molecules were positively charged. The constant adsorption capacity of activated carbon for dyes with the pH ≥ 9 was an indication that the electrostatic mechanism was not the only mechanism for dye adsorption in this system. Activated carbon can also interact with dye molecules via hydrogen bonding and hydrophobic-hydrophobic mechanisms [30].

In order to describe the competitive adsorption, we used the intra particle diffusion model proposed by Weber and Morris [31]. In a liquid-solid system, the fractional uptake of the solute on a particle varies according to r (the particle radius) and a fraction of D (the diffusivity within the particle). The initial rate of the intra particle diffusion was obtained by linearization of the curve $qt = f(t^{1/2})$. The plot of qt against $t^{1/2}$ may present multi-linearity [32]. This shows that two or more steps occur in the adsorption processes. The first sharper portion is instantaneous adsorption stage or external surface adsorption. The second portion presents the gradual adsorption stage; in this stage the intra particle diffusion is rate-controlled. The third portion presents the final equilibrium stage in which the intra particle diffusion starts to slow down because of a low solute concentration in the solution.

The comparison of the diffusion rate constants $k_{int\text{-}1}$ and $k_{int\text{-}2}$, for the same adsorbent, shows that $k_{int\text{-}2}$ = 3.83 (stage 2) has a lower value than $k_{int\text{-}1}$ = 7.17 (stage 1) for both adsorbents.

The reduction of the adsorption rate in the second stage may be due to pore blockage or steric hin-

drance exerted by the adsorbed MB onto the adsorbent surface. As shown by Fig. 5, the plots of *qt* vs $t^{1/2}$ did not fit with straight lines passing through the origin as required by Eq. (1), indicating the inapplicability of this model, and the intra particle diffusion was not the rate-controlling step during the adsorption process of MB ions onto AC:

$$q_t = K_{int} \cdot t^{1/2} + C, \quad (1)$$

where K_{int} is the intraparticle diffusion rate constant (mg/g·h$^{1/2}$) and *C* is the intercept (mg/g) proportional to the boundary layer thickness.

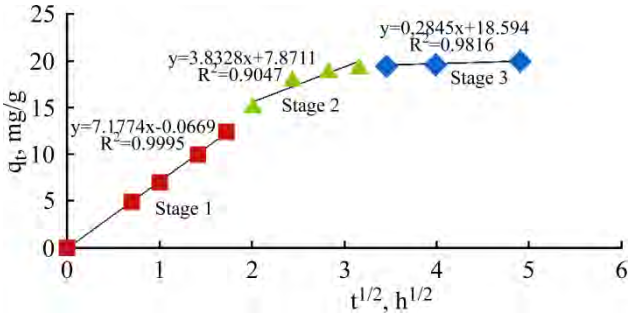

Fig. 5. Intra particle diffusion plots for MB adsorption onto activated carbon.

CONCLUSION

The results of this work can be summarized as follows:

(1) The N_2 adsorption isotherm on activated carbon is of type I. The values of S_{BET}, S_{micro}, V_t and V_{mic} are 600 m^2/g, 492 m^2/g, 0.39 cm^3/g and 0.26 cm^3/g, respectively. Results show that activated carbon is dominantly micropores. Percentage of micropores area is 82%.

(2) The maximum removal of the dye was observed at pH = 9. Adsorption experiments were carried out for different contact times at different temperatures with a fixed adsorbent dosage of 0.1 g/50 mL at natural pH. The equilibrium time was 6 h.

(3) The adsorption isotherm followed the Langmuir and Freundlich models. The Langmuir model gave a better fit to all adsorption isotherms than the Freundlich one.

(4) The kinetics of adsorption of MB onto natural lignite and corresponding activated carbon was studied by using two kinetic models. The adsorption of MB from aqueous solution onto the microporous activated carbon proceeds according to the pseudo-second-order model which provides the best correlation of the data in all cases.

REFERENCES

1. Mahmoudi K., Hamdi N., Kriaa A., Srasra E. Adsorption of Methyl Orange using Activated Carbon Prepared from Lignin by $ZnCl_2$ Treatment. *Russ J Phys Ch A.* 2012, **86**(8), 1294–1300. *doi: 10.1134/S0036024412060180.*
2. Feng-Chin W., Pin-Hsueh W., Ru-Ling T., Ruey-Shin J. Preparation of Novel Activated Carbons from H_2SO_4-Pretreated Corncob Hulls with KOH Activation for Quick Adsorption of Dye and 4-chlorophenol. *J Environ Manage.* 2011, **92**(3), 708–713. *doi: 10.1016/j.jenvman.2010.10.003*
3. Prahas D., Kartika Y., Indraswati N., Ismadji S. Activated Carbon from Jackfruit Peel Waste by H_3PO_4 Chemical Activation: Pore Structure and Surface Chemistry Characterization. *Chemical Engineering J.* 2008, **140**(1–3), 32–42. *doi: 10.1016/j.cej.2007.08.032*
4. Mestre A.S., Bexiga A.S., Proença M., Andrade M., Pinto M.L., Matos I., Fonseca I.M., Carvalho A.P. Activated Carbons from Sisal Waste by Chemical Activation with K_2CO_3: Kinetics of Paracetamol and Ibuprofen Removal from Aqueous Solution. *Bioresource Technol.* 2011, **102**(17), 8253–8260. *doi: 10.1016/j.biortech.2011.06.024*
5. Ferrera-Lorenzo N., Fuente E., Suárez-Ruiz I., Ruiz B. KOH Activated Carbon from Conventional and Microwave Heating System of a Macro Algae Waste from the Agar–Agar industry. *Fuel Process. Technol.* 2014, **121**, 25–31. *doi: 10.1016/j.fuproc.2013.12.017*
6. Cazetta A.L., Vargas A.M.M., Nogami E.M., Kunita M.H., Guilherme M.R., Martins A.C., Silva T.L., Moraes J.C.G., Almeida V.C. NaOH-activated Carbon of High Surface Area Produced from Coconut Shell: Kinetics and Equilibrium Studies from the Methylene Blue Adsorption. *Chem Eng J.* 2011, **174**(1), 117–125. *doi: 10.1016/j.cej.2011.08.058*
7. Wigmans T., Doorn J. van, Moulijn J.A. Temperature-programmed Desorption Study of Na_2CO_3-containing Activated Carbon. *Fuel.* 1983, **62**(2), 190–195. *doi: 10.1016/0016-2361(83)90196-5*
8. Pin G., Zhen-hong L., Gang X., Bin H., Mei-hua Z. Preparation and Characterization of Activated Carbon Produced from Rice Straw by $(NH_4)_2HPO_4$ Activation. *Bioresource Technol.* 2011, **102**(3), 3645–3648. *doi: 10.1016/j.biortech.2010.11.080*
9. Reha Y., Hanife A., Nilgün K., Eda C. Influence of Preparation Conditions on Porous Structures of Olive Stone Activated by H_3PO_4. *Fuel Process. Technol.* 2010, **91**, 80–87.
10. Bouchelta C., Medjram M.S., Zoubida M., Chekkat F. Ahmed, Ramdane N., Bellat J.P. Effects of Pyrolysis Conditions on the Porous Structure Development of Date Pits Activated Carbon. *J Anal Appl Pyrol.* 2012, **94**, 215–222.
11. Dastgheib S.A., Rockstraw D.A. A Model for the Adsorption of Single Metal Ion Solutes in Aqueous Solution onto Activated Carbon Produced from Pecan Shells. *Carbon.* 2002, **40**, 1843–1851.
12. Rodríguez-Reinoso F. An Overview of Methods for the Characterization of Activated Carbons. *Pure Appl. Chem.* 1989, **61**, 1859–1866.

13. Dinesh M., Ankur S., Singh V.K., Alexandre-Franco M., Pittman C.U. Development of Magnetic Activated Carbon from Almond Shells for Trinitrophenol Removal from Water. *Chem. Eng. J.* 2011, **172**, 1111–1125.

14. Noh J.S., Schwarz J.A. Estimation of the Point of Zero Charge of Simple Oxides by Mass Titration. *J Colloid Interf Sci*. 1989, **130**, 157–164.

15. Boehm H.P. Chemical Identification of Surface Groups. *Adv. Catal*. 1966, **16**, 179–274.

16. Boehm H.P. Some Aspects of the Surface Chemistry of Carbon Blacks and other Carbons. *Carbon*. 1994, **32**, 759–769.

17. Papier E., Li S., Donnet J.-B. Contribution to the Study of Basic Surface Groups on Carbons. *Carbon*. 1987, **25**, 243–247. *doi: 10.1016/0008-6223(87) 90122-9*

18. Maldhure A.V., Ekhe J. Preparation and Characterizations of Microwave Assisted Activated Carbons from Industrial Waste Lignin for Cu (II) Sorption. *Chem Eng J.* 2011, **168**(3), 1103–1111. *doi: 10.1016/j.cej.2011.01.09*

19. San Miguel G., Fowler G.D., Sollars C.J. A Study of the Characteristics of Activated Carbons Produced by Steam and Carbon Dioxide Activation of Waste Tyre Rubber. *Carbon*. 2003, **41**, 1009–1016. *doi: 10.1016/S0008-6223(02)00449-9*

20. Langmuir I. The Constitution and Fundamental Properties of Solids and Liquids. Part I. Solids. *J Am Chem Soc*. 1916, **38**(11), 2221–2295. *doi: 10.1021/ ja02268a002*

21. Freundlich H.M.F. Uber Die Adsorption in Losungen. *Z Phys Chem*. 1906, **57**(A), 385–470.

22. Lagergren S. *Zur Theorie der sogenannten Adsorption gelöster Stoffe*. Bihang till K. Sven. Vetenskapsakad. Handl**.** 1898, Bd 24:Afd.2: no 4, 39 p.

23. Ho Y.S., McKay G. Kinetic Models for the Sorption of Dye from Aqueous Solution by Wood. *Trans IChemE*, 1998, **76**(B), 183–191.

24. Sing K.S.W. Reporting Physisorption Data for Gas/ Solid Systems with Special Reference to the Determination of Surface Area and porosity (Recommendations 1984). *Pure Appl Chem.* 2009, **57**(4), 603–619. *doi: 10.1351/pac198557040603*

25. Pavan F.A., Mazzocato A.C., Gushikem Y. Removal of Methylene Blue Dye from Aqueous Solutions by Adsorption using Yellow Passion Fruit Peel as Adsorbent. *Bioresource Technol*. 2008, **99**, 3162–3165. *doi: 10.1016/j.biortech.2007.05.067*

26. Gurses A., Dogar C., Yalcina M., Acikyildiz M., Bayrak R., Karaca S. The Adsorption Kinetics of the Cationic Dye, Methylene Blue, onto Clay. *J Hazard Mater B.* 2006, **131**, 217–228. *doi: 10.1016/ j.jhazmat.2005.09.036*

27. Auta M., Hameed B.H. Coalesced Chitosan Activated Carbon Composite for Batch and Fixed-bed Adsorption of Cationic and Anionic Dyes. *Colloid Surface B.* 2013, **105**, 199–206. *doi: 10.1016/j.colsurfb. 2012.12.021*

28. Lei Yu, Yong-ming Luoa. The Adsorption Mechanism of Anionic and Cationic Dyes by Jerusalem Artichoke Stalk-based Mesoporous Activated Carbon. *JECE*. 2014, **2**(1), 220–229. *doi: 10.1016/j.jece. 2013.12.016*

29. Rodríguez A., García J., Ovejero G.l, Mestanza M. Adsorption of Anionic and Cationic Dyes on Activated Carbon from Aqueous Solutions: Equilibrium and Kinetics. *J Hazard Mater.* 2009, **172**(2–3), 1311–1320. *doi: 10.1016/j.jhazmat.2009.07.138.*

30. Newcombe G., Drikas M. Adsorption of NOM Activated Carbon: Electrostatic and Non-electrostatic Effects. *Carbon*. 1997, **35**, 1239–1250. *doi: 10.1016/ S0008-6223(97)00078-X*

31. Weber W.J., Morris J.C. Kinetics of Adsorption on Carbon from Solution. *J of the Sanitary Engineering Division.* 1963, **89**(2), 31–60.

32. Allen S.J., McKay G., Khader K.Y.H. Intraparticle Diffusion of a Basic Dye during Adsorption onto Sphagnum Peat. *Environ Pollut*. 1989, **56**(1), 39–50. *doi: 10.1016/0269-7491(89)90120-6*

Received 25.08.14
Accepted 17.11.14

Реферат

Адсорбент был получен из лигнита при химической активации с помощью $ZnCl_2$. Свойства пор активированного угля, такие как площадь поверхности, определяемая по методу *Брунауэра-Эммета-Теллера (БЭТ)*, объем пор, распределение пор по размерам, и диаметр пор характеризовались по *t*-кривой на основе изотермы адсорбции N_2. Первичная площадь поверхности адсорбента, определяемая микропорами, была 600 $м^2$/г. Активированный уголь из лигнита использовали для адсорбции метиленового синего (МС) из водного раствора. Было изучено влияние концентрации исходного красителя, времени перемешивания и начального pH. Было установлено, что изотермы адсорбции согласуются с обеими моделями Ленгмюра и Фрейндлиха. Тем не менее, модель Ленгмюра лучше подходят для всех изотерм адсорбции, чем модель Фрейндлиха. Кинетика адсорбции МС была проверена с помощью моделей псевдо-первого порядка, псевдо-второго порядка, а также уравнения внутренней диффузии частиц. Полученные результаты показывают, что адсорбция МС из водного раствора на микропористом активированном угле происходит в соответствии с моделью псевдо-второго порядка.

Ключевые слова: активированный уголь, лигнит, адсорбция, метиленовый синий.